Letter

First observation of $\Lambda_b^0 \to \Sigma_c^{(*)++} D^{(*)-} K^-$ decays

R. Aaij *et al.*[*]
(LHCb Collaboration)

(Received 3 May 2024; accepted 6 June 2024; published 22 August 2024)

The four decays, $\Lambda_b^0 \to \Sigma_c^{(*)++} D^{(*)-} K^-$, are observed for the first time using proton-proton collision data collected with the LHCb detector at a center-of-mass energy of 13 TeV, corresponding to an integrated luminosity of 6 fb^{-1}. By considering the $\Lambda_b^0 \to \Lambda_c^+ \bar{D}^0 K^-$ decay as reference channel, the following branching fraction ratios are measured to be $\frac{\mathcal{B}(\Lambda_b^0 \to \Sigma_c^{++} D^- K^-)}{\mathcal{B}(\Lambda_b^0 \to \Lambda_c^+ \bar{D}^0 K^-)} = 0.282 \pm 0.016 \pm 0.016 \pm 0.005$, $\frac{\mathcal{B}(\Lambda_b^0 \to \Sigma_c^{*++} D^- K^-)}{\mathcal{B}(\Lambda_b^0 \to \Sigma_c^{++} D^- K^-)} = 0.460 \pm 0.052 \pm 0.028$, $\frac{\mathcal{B}(\Lambda_b^0 \to \Sigma_c^{++} D^{*-} K^-)}{\mathcal{B}(\Lambda_b^0 \to \Sigma_c^{++} D^- K^-)} = 2.261 \pm 0.202 \pm 0.129 \pm 0.046$, $\frac{\mathcal{B}(\Lambda_b^0 \to \Sigma_c^{*++} D^{*-} K^-)}{\mathcal{B}(\Lambda_b^0 \to \Sigma_c^{++} D^- K^-)} = 0.896 \pm 0.137 \pm 0.066 \pm 0.018$, where the first uncertainties are statistical, the second are systematic, and the third are due to uncertainties in the branching fractions of intermediate particle decays. These initial observations mark the beginning of pentaquark searches in these modes, with more datasets to become available following the LHCb upgrade.

DOI: 10.1103/PhysRevD.110.L031104

Introduction. The existence of exotic pentaquark states, comprising four quarks and an antiquark, has been predicted since the establishment of the quark model [1]. The search for pentaquark candidates has been performed by many experiments in the past 50 years [2–4] but only the LHCb experiment has given conclusive results. In 2015, the LHCb experiment reported the observation of $J/\psi p$ resonant structures [5,6], consistent with pentaquark candidates made up of minimal quark content $c\bar{c}uud$, produced in $\Lambda_b^0 \to J/\psi p K^-$ decays.[1] An amplitude analysis showed that the data is best described with the inclusion of two pentaquark states, the $P_\psi^N(4380)^+$ and $P_\psi^N(4450)^+$. With additional data and an improved selection strategy, it was found that the $P_\psi^N(4450)^+$ structure resolves into two narrower substructures, the $P_\psi^N(4440)^+$ and $P_\psi^N(4457)^+$. In addition, a new narrow pentaquark candidate, the $P_\psi^N(4312)^+$, was discovered [7].

The newly observed exotic candidates have masses less than 10 MeV below the $\Sigma_c \bar{D}^{(*)}$ thresholds.[2] The proximity of the pentaquark candidates to open-charm thresholds, as well as their very narrow widths, favor the loosely bound (so-called molecular) pentaquark model, in which the $\bar{D}^{(*)}$ meson and the $\Sigma_c^{(*)}$ baryon are bound by a residual strong force similar to that binding a proton and neutron to form a deuteron [8]. In addition, several molecular pentaquark models predict that a P_ψ^{N+} with $3/2^-$ spin parity would decay substantially into $\Sigma_c^{(*)} \bar{D}$ [9–12]. This motivates the search for $\Lambda_b^0 \to \Sigma_c^{(*)++} D^{(*)-} K^-$ decays,[3] whose tree-level Feynman diagrams, shown in Fig. 1 (left), are color suppressed but not forbidden [13]. The topologically similar $\Lambda_b^0 \to \Lambda_c^+ \bar{D}^0 K^-$ process is chosen as the reference mode, which has contributions from both color-suppressed and color-favored tree-level diagrams. As shown in Fig. 1 (right) for the color-favored process, the spectator quarks (ud) of the Λ_b^0 baryon directly propagate into the charmed baryon (udc), which must preserve the isospin-0 quantum number of the parent Λ_b^0 baryon, and thus be a Λ_c^+ state.

This article presents the search for four new $\Lambda_b^0 \to \Sigma_c^{(*)++} D^{(*)-} K^-$ decay modes using proton-proton (pp) collision data collected by the LHCb experiment at a center-of-mass energy of 13 TeV during the Run 2 data-taking period from 2015 to 2018, corresponding to an integrated luminosity of 6 fb^{-1}. The relative branching fractions, $\frac{\mathcal{B}(\Lambda_b^0 \to \Sigma_c^{++} D^- K^-)}{\mathcal{B}(\Lambda_b^0 \to \Lambda_c^+ \bar{D}^0 K^-)}$, $\frac{\mathcal{B}(\Lambda_b^0 \to \Sigma_c^{*++} D^- K^-)}{\mathcal{B}(\Lambda_b^0 \to \Sigma_c^{++} D^- K^-)}$, $\frac{\mathcal{B}(\Lambda_b^0 \to \Sigma_c^{++} D^{*-} K^-)}{\mathcal{B}(\Lambda_b^0 \to \Sigma_c^{++} D^- K^-)}$, and $\frac{\mathcal{B}(\Lambda_b^0 \to \Sigma_c^{*++} D^{*-} K^-)}{\mathcal{B}(\Lambda_b^0 \to \Sigma_c^{++} D^- K^-)}$ are measured. Given that the decay modes in the last three ratios have the same number of final tracks and final states similar to those of the

[*]Full author list given at the end of the article.

[1]Inclusion of charge-conjugate processes is implied throughout.

[2]Natural units with $\hbar = c = 1$ are used throughout.

[3]The symbols Σ_c^{++} and Σ_c^{*++} refer to $\Sigma_c(2455)^{++}$ and $\Sigma_c(2520)^{++}$.

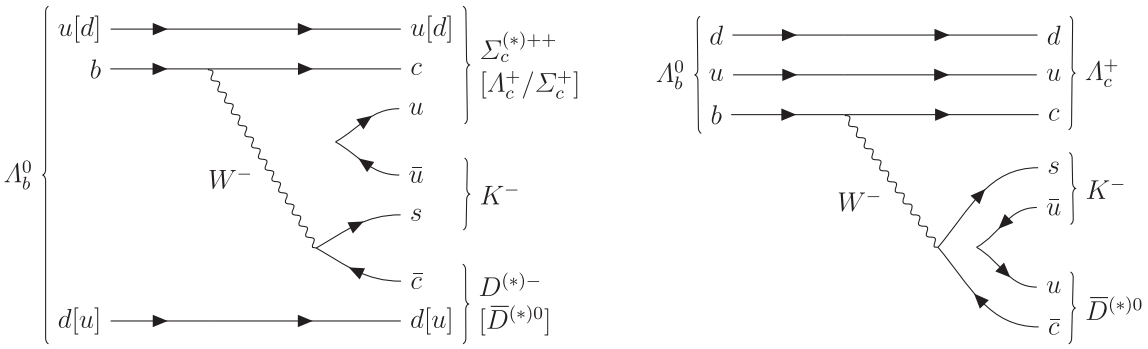

FIG. 1. Feynman diagrams for (left) color-suppressed and (right) color-favored tree processes of the Λ_b^0 baryon decaying into $\Sigma_c^{(*)}\bar{D}^{(*)}K^-$ or $\Lambda_c^+\bar{D}^{(*)0}K^-$.

$\Lambda_b^0 \to \Sigma_c^{++}D^-K^-$ decay mode, their relative branching fractions with respect to the $\Lambda_b^0 \to \Sigma_c^{++}D^-K^-$ decay are measured to facilitate the cancellation of several systematic uncertainties due to the effects from detector acceptance, triggers, and tracking.

Detector and simulation. The LHCb detector [14,15] is a single-arm forward spectrometer covering the pseudorapidity range $2 < \eta < 5$, designed for the study of particles containing b or c quarks. The detector elements that are particularly relevant to this analysis are a silicon-strip vertex detector surrounding the pp interaction region that allows c and b hadrons to be identified from their characteristically long flight distance; a tracking system that provides a measurement of the momentum, p, of charged particles; and two ring-imaging Cherenkov detectors that are able to discriminate between different species of charged hadrons.

The online event selection is performed by a trigger [16], which consists of a hardware and a software stage. At the hardware stage, events are required to have a muon with high transverse momentum, p_T, or a hadron, photon, or electron with high transverse energy in the calorimeters. The triggered objects can be either hadrons from the Λ_b^0 decays of interest [trigger on signal, (TOS)] or any particle from the rest of the event [trigger independently of signal, (TIS)]. The software trigger applies a full event reconstruction, and subsequently requires at least one charged particle from the event to have a larger p_T and be inconsistent with originating from any reconstructed primary pp interaction vertex (PV). Furthermore, the reconstructed events must have signal candidates forming a two-, three-, or four-track secondary vertex significantly displaced from any PV. The secondary vertices are filtered by a multivariate algorithm [17] to be consistent with the decay of a beauty hadron.

Simulation is required to model the resolution effects of event reconstruction and to calculate the efficiencies due to detector acceptance and selection requirements. In the simulation, pp collisions are generated using PYTHIA [18] with a specific LHCb configuration [19]. Decays of unstable particles are described by EvtGen [20], in which final-state radiation is generated using PHOTOS [21]. The interaction of the generated particles with the detector, and its response, are implemented using the Geant4 toolkit [22] as described in Ref. [23]. The particle-identification (PID) response is not well described in the LHCb simulation and is corrected to match that in data using dedicated calibration samples. The corrections are based on a four-dimensional kernel density estimation for distributions in the PID response, p_T and η of the track, and the multiplicity of the event [24].

Candidate selection. The $\Lambda_b^0 \to \Sigma_c^{(*)++}D^{(*)-}K^-$ candidates are reconstructed through the decay chains $\Sigma_c^{(*)++} \to \Lambda_c^+\pi^+$ with $\Lambda_c^+ \to pK^-\pi^+$ and $D^- \to K^+\pi^-\pi^-$ or $D^{*-} \to \bar{D}^0\pi^-$ with $\bar{D}^0 \to K^+\pi^-$. The reconstructed final-state particles are required to have PID information consistent with their respective mass hypotheses and be inconsistent with originating from any PV. At least one of them must have $p > 10$ GeV and $p_T > 1.7$ GeV. Each of the Λ_c^+, $\bar{D}^0$, and $D^{(*)-}$ decay vertices must have a good vertex-fit quality and be significantly displaced from its associated PV, defined as the primary vertex that fits best to the flight direction of the candidate. The reconstructed masses of the charmed hadron candidates must be consistent with their known values [25], within 15 MeV for the Λ_c^+ baryon and 25 MeV for the charmed mesons. Subsequently, the Λ_b^0 candidate is reconstructed by combining Λ_c^+, $D^{(*)-}$, K^- and π^+ candidates to form a good vertex. The momentum vector of the Λ_b^0 candidate is required to be consistent with the flight direction. The sum of transverse momentum of the Λ_b^0 decay products must be greater than 5 GeV and the decay time of the Λ_b^0 candidate is required to be greater than 0.2 ps. Clone tracks are pairs of reconstructed tracks that share a majority of their detector hits. They are rejected by requiring the opening angle between any pair of final-state tracks from the Λ_b^0 candidate to be greater than 0.5 mrad. The reference

channel $\Lambda_b^0 \to \Lambda_c^+ \bar{D}^0 K^-$ is reconstructed from the same Λ_c^+ and $\bar{D}^0$ decay channels by applying the same selections.

Non-negligible peaking backgrounds in the signal and reference channels result from Λ_b^0 decays to the same final state but without one or both intermediate charm hadrons. These are denoted by non-doubly-charmed (NDC) backgrounds. Genuine Λ_c^+ and $\bar{D}^0$ (D^-) hadrons have nonzero lifetimes and decay at tertiary vertices in the forward direction with respect to the Λ_b^0 baryon decay vertex. To suppress this background, the separation along the beam direction z between the charmed hadrons and the Λ_b^0 decay vertex is required to be greater than -1 mm and its significance must be greater than 1, -2.5, -1.5, and -2.0 for D^- in signal decay, Λ_c^+ in signal decay, $\bar{D}^0$ in reference decay, and Λ_c^+ in reference decay, respectively. The negative values of these requirements account for the limited resolution of the vertex reconstruction.

Specific backgrounds from misreconstructed or misidentified particles are vetoed by applying selections on the invariant masses. A misreconstructed background can arise from the two final-state kaons being correctly identified but assigned to the wrong Λ_c^+ and Λ_b^0 parent particles. Therefore, peaks in $\Lambda_c^+ \to (p\pi^+)_{\Lambda_c^+} K^-_{\Lambda_b^0}$ are vetoed, where the subscript in each final state particle denotes the assumed parent during reconstruction.

For misidentified backgrounds, the vetoes are applied by assigning an alternative mass hypothesis to the final state particles, and rejecting candidates that have a recalculated invariant mass consistent with known resonances. Misidentified background vetoes are applied for $D_s^+ \to (\{K^+ \Rightarrow p\}K^-\pi^+)_{\Lambda_c^+}$, $\phi \to (\{K^+ \Rightarrow p\}K^-)_{\Lambda_c^+}$, $\phi \to \{K^+ \Rightarrow p\}_{\Lambda_c^+} K^-_{\Lambda_b^0}$, $D^0 \to (K^-\{\pi^+ \Rightarrow p\})_{\Lambda_c^+}$, $\Lambda_c^+ \to (p\pi^+)_{\Lambda_c^+}\{K^- \Rightarrow \pi^-\}_{\bar{D}^0/D^-}$, and $D^{*-} \to \bar{D}^0_{\Lambda_b^0}\{\pi^- \Rightarrow K^-\}_{\Lambda_b^0/\Lambda_c^+}$ decays,[4] where the subscript denotes the parent assumed during reconstruction. The last veto is only applied to decay chains with a $\bar{D}^0$ meson, while the others are applied to all decay modes.

After applying all selections, a few percent of events contain multiple candidates. These are mostly due to duplicated use of the same tracks. In such events, the candidate with the smallest value of χ^2 from a kinematic fit with constrained decay vertices is retained.

Mass fit. The yields of the $\Lambda_b^0 \to \Sigma_c^{(*)++} D^- K^-$ ($\Lambda_b^0 \to \Sigma_c^{(*)++} D^{*-} K^-$) signal decays are determined from unbinned two-dimensional maximum likelihood fits to the $m_{\Lambda_c^+\pi^+}$ and $m_{\Lambda_c^+ D^- K^-\pi^+}$ ($m_{\Lambda_c^+ D^{*-} K^-\pi^+}$) invariant mass distributions, where the subscript denotes the particle combination used to calculate the invariant masses. The $m_{\Lambda_c^+\pi^+}$ dimension is used to disentangle the contributions from Σ_c^{++}, Σ_c^{*++} and nonresonant $\Lambda_c^+\pi^+$. To reduce the correlation between $m_{\Lambda_c^+\pi^+}$ and $m_{\Lambda_c^+ D^- K^-\pi^+}$ ($m_{\Lambda_c^+ D^{*-} K^-\pi^+}$) and improve the resolution of their mass spectra, the invariant mass $m_{\Lambda_c^+\pi^+}$ is reconstructed by a kinematic fit which requires the Λ_b^0 to originate from its associated PV and constrains the Λ_b^0, Λ_c^+ and D^- (D^{*-}) to their known masses [25]. The same PV constraint is also applied when reconstructing $m_{\Lambda_c^+ D^- K^-\pi^+}$ ($m_{\Lambda_c^+ D^{*-} K^-\pi^+}$) but only the Λ_c^+ and D^- (D^{*-}) masses are constrained.

Both two-dimensional fits contain six components each. The signal decays $\Lambda_b^0 \to \Sigma_c^{(*)++} D^- K^-$ and $\Lambda_b^0 \to \Sigma_c^{(*)++} D^{*-} K^-$ include a resonant $\Sigma_c^{(*)++}$ and a peaking Λ_b^0 component. The resonant $\Sigma_c^{(*)++}$ distribution is modeled by an incoherent relativistic Breit-Wigner distribution convolved with a Gaussian resolution function. The Breit-Wigner masses and widths of the $\Sigma_c^{(*)++}$ state are fixed to their known values [25], while the detector resolution is obtained from simulation. The Λ_b^0 mass peak is modeled by the sum of two Crystal Ball [26] functions, one with a low-mass tail and the other with a high-mass tail. The two functions share a common mean. For each decay mode, the shape parameters are determined from fits to simulation, except for the mean and a width scale factor which are free parameters in the data fit to account for imperfections in the simulation.

A purely combinatorial background component is described by a threshold function in $m_{\Lambda_c^+\pi^+}$ and an exponential function in $m_{\Lambda_c^+ D^- K^-\pi^+}$ ($m_{\Lambda_c^+ D^{*-} K^-\pi^+}$), whose parameters are determined from data. Two background components with resonant $\Sigma_c^{(*)++}$ states but nonpeaking in the Λ_b^0 invariant mass share the $\Sigma_c^{(*)++}$ shape parameters with the signal modes and share the $m_{\Lambda_c^+ D^- K^-\pi^+}$ ($m_{\Lambda_c^+ D^{*-} K^-\pi^+}$) exponential slope with each other, but not with the pure combinatorial background. A peaking Λ_b^0 background component with nonresonant $\Lambda_c^+\,\pi^+$ shares the peaking Λ_b^0 shape parameters with the signal modes and shares the $m_{\Lambda_c^+\pi^+}$ threshold function parameters with the pure combinatorial background.

The one-dimensional projections of both fits are shown in Fig. 2. The obtained yields are 480 ± 25 for $\Lambda_b^0 \to \Sigma_c^{++} D^- K^-$, 279 ± 26 for $\Lambda_b^0 \to \Sigma_c^{*++} D^- K^-$, 243 ± 17 for $\Lambda_b^0 \to \Sigma_c^{++} D^{*-} K^-$ and 116 ± 15 for $\Lambda_b^0 \to \Sigma_c^{*++} D^{*-} K^-$ signal decays. These results are tested for stability by generating and fitting 3000 pseudoexperiments with the default model described above, and no significant bias was observed.

The yield of the $\Lambda_b^0 \to \Lambda_c^+ \bar{D}^0 K^-$ reference mode is determined by a one-dimensional fit to $m_{\Lambda_c^+ \bar{D}^0 K^-}$. Similar to the treatment of the signal decay modes, $m_{\Lambda_c^+ \bar{D}^0 K^-}$ is reconstructed by constraining the Λ_b^0 candidate to originate

[4]The particle species on the left and right of the arrow ($\Rightarrow$) correspond to the alternative and default mass hypotheses, respectively.

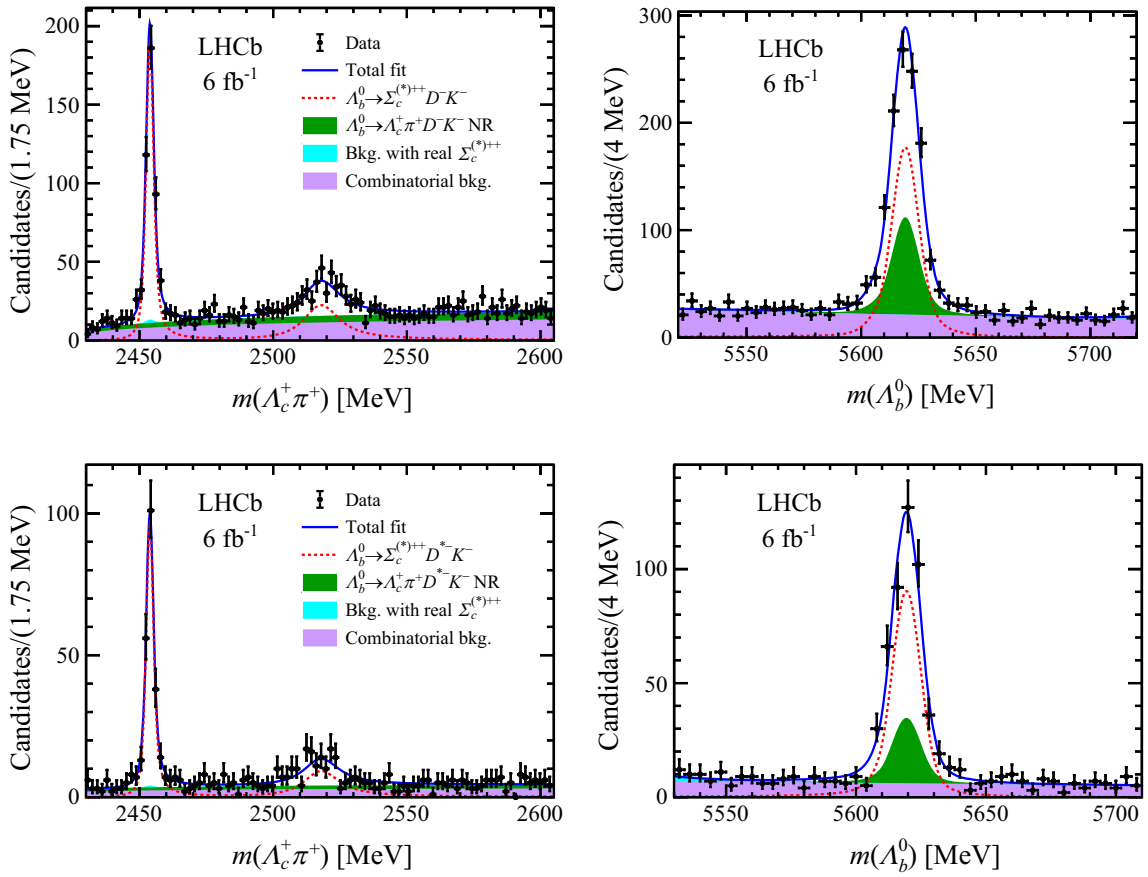

FIG. 2. Two-dimensional invariant mass fits of the $\Lambda_b^0 \to \Sigma_c^{(*)++} D^- K^-$ decay, projected onto (top left) $m_{\Lambda_c^+\pi^+}$ and (top right) $m_{\Lambda_c^+ D^- K^- \pi^+}$. A similar fit to $\Lambda_b^0 \to \Sigma_c^{(*)++} D^{*-} K^-$ decay is projected onto (bottom left) $m_{\Lambda_c^+\pi^+}$ and (bottom right) $m_{\Lambda_c^+ D^{*-} K^- \pi^+}$. The two signal contributions with resonant Σ_c^{++} and Σ_c^{*++} are drawn as a single component (red dashed line). Similarly, the two resonant $\Sigma_c^{(*)++}$ backgrounds without Λ_b^0 peaks are drawn together (cyan fill).

from its associated PV and applying mass constraints to the intermediate Λ_c^+ and $\bar{D}^0$ particles to improve the mass resolution. For both signal and background components, the Λ_b^0 candidate spectrum is modeled in the same way as for the signal. The fitted yield of the $\Lambda_b^0 \to \Lambda_c^+ \bar{D}^0 K^-$ reference decay is 4032 ± 75.

Ratio of branching fractions. The yields of the signal and reference modes are corrected for the Dalitz distribution of the Λ_b^0 decay by considering per-event efficiencies,

$$N_{\rm corr} = \sum_i \frac{s\mathcal{W}_i}{\epsilon(s_i^{12}, s_i^{13})} \tag{1}$$

where $N_{\rm corr}$ is the corrected yield, $s\mathcal{W}_i$ is the per-event signal weight from the *sPlot* method [27] and the efficiency, $\epsilon(s_i^{12}, s_i^{13})$, is calculated event-by-event based on the Dalitz variables s^{12} and s^{13}. These Dalitz variables represent the square of the invariant mass of $\Sigma_c^{(*)++} D^{(*)-}$ system and $\Sigma_c^{(*)++} K^-$ system in the three-body decay of the Λ_b^0 baryon. The efficiency is obtained using Λ_b^0 decays with uniform distribution over the phase space and applying the candidate selection.

Given the corrected yields $N_{\rm corr}$, the ratios of branching fractions are calculated via

$$\frac{\mathcal{B}(\Lambda_b^0 \to \Sigma_c^{++} D^- K^-)}{\mathcal{B}(\Lambda_b^0 \to \Lambda_c^+ \bar{D}^0 K^-)} = \frac{N_{\rm corr}(\Lambda_b^0 \to \Sigma_c^{++} D^- K^-)}{N_{\rm corr}(\Lambda_b^0 \to \Lambda_c^+ \bar{D}^0 K^-)} \cdot \frac{\mathcal{B}(\bar{D}^0 \to K^+\pi^-)}{\mathcal{B}(D^- \to K^+\pi^-\pi^-)}, \tag{2}$$

$$\frac{\mathcal{B}(\Lambda_b^0 \to \Sigma_c^{*++} D^- K^-)}{\mathcal{B}(\Lambda_b^0 \to \Sigma_c^{++} D^- K^-)} = \frac{N_{\rm corr}(\Lambda_b^0 \to \Sigma_c^{*++} D^- K^-)}{N_{\rm corr}(\Lambda_b^0 \to \Sigma_c^{++} D^- K^-)}, \tag{3}$$

$$\frac{\mathcal{B}(\Lambda_b^0 \to \Sigma_c^{++} D^{*-} K^-)}{\mathcal{B}(\Lambda_b^0 \to \Sigma_c^{++} D^- K^-)} = \frac{N_{\rm corr}(\Lambda_b^0 \to \Sigma_c^{++} D^{*-} K^-)}{N_{\rm corr}(\Lambda_b^0 \to \Sigma_c^{++} D^- K^-)} \cdot \frac{\mathcal{B}(D^- \to K^+\pi^-\pi^-)}{\mathcal{B}(D^{*-} \to \bar{D}^0\pi^-)\mathcal{B}(\bar{D}^0 \to K^+\pi^-)}, \tag{4}$$

$$\frac{\mathcal{B}(\Lambda_b^0 \to \Sigma_c^{*++} D^{*-} K^-)}{\mathcal{B}(\Lambda_b^0 \to \Sigma_c^{++} D^- K^-)} = \frac{N_{\rm corr}(\Lambda_b^0 \to \Sigma_c^{*++} D^{*-} K^-)}{N_{\rm corr}(\Lambda_b^0 \to \Sigma_c^{++} D^- K^-)} \cdot \frac{\mathcal{B}(D^- \to K^+ \pi^- \pi^-)}{\mathcal{B}(D^{*-} \to \bar{D}^0 \pi^-)\mathcal{B}(\bar{D}^0 \to K^+ \pi^-)}, \tag{5}$$

where the branching fractions ($\mathcal{B}$) of charmed mesons assume the values published in Ref. [25]. The $\Sigma_c^{(*)++} \to \Lambda_c^+ \pi^+$ decays are not considered in the formulas above because they are the only strong processes allowed by the mass threshold limit, and their branching fractions are assumed to be unity.

Systematic uncertainties. The four signal decay channels have the same final state and similar decay topologies, hence the systematic uncertainties from the modeling of track reconstruction efficiency in the simulation are assumed to cancel out in the efficiency ratios. This cancellation does not apply between $\Lambda_b^0 \to \Lambda_c^+ \bar{D}^0 K^-$ (reference) and $\Lambda_b^0 \to \Sigma_c^{++} D^- K^-$ (signal) decays because the latter has two extra pions and an intermediate Σ_c^{++}. The modeling of the track reconstruction efficiency in simulation results in a systematic uncertainty of 1.61% for each extra pion in the $\Lambda_b^0 \to \Sigma_c^{++} D^- K^-$ decays due to the imperfect simulation of hadronic interactions with the detector material [28].

Similarly, imperfections in hardware trigger efficiencies between signal modes are assumed to cancel out in the efficiency ratios, but not in the ratio between $\Lambda_b^0 \to \Lambda_c^+ \bar{D}^0 K^-$ and $\Lambda_b^0 \to \Sigma_c^{++} D^- K^-$ decays. To correct for this, the TIS-TOS method [16] is used to derive data-driven corrections to the simulated values. Such factors are binned in maximum $p_{\rm T}$ of the final state particles, for both the $\Lambda_b^0 \to \Lambda_c^+ \bar{D}^0 K^-$ and $\Lambda_b^0 \to \Sigma_c^{++} D^- K^-$ decays. By default, the correction table derived from $\Lambda_b^0 \to \Lambda_c^+ \bar{D}^0 K^-$ decays is used to correct the $\Lambda_b^0 \to \Lambda_c^+ \bar{D}^0 K^-$ simulation, and likewise when correcting the $\Lambda_b^0 \to \Sigma_c^{++} D^- K^-$ simulation. As a systematic, only a single correction table is used to correct both decay modes, or the correction factors derived from $\Lambda_b^0 \to \Lambda_c^+ \bar{D}^0 K^-$ and $\Lambda_b^0 \to \Sigma_c^{++} D^- K^-$ decays are used to correct $\Lambda_b^0 \to \Sigma_c^{++} D^- K^-$ and $\Lambda_b^0 \to \Lambda_c^+ \bar{D}^0 K^-$ simulation respectively. The largest change in the efficiency ratio between $\Lambda_b^0 \to \Lambda_c^+ \bar{D}^0 K^-$ and $\Lambda_b^0 \to \Sigma_c^{++} D^- K^-$ decays is 0.77%, which is assigned as the systematic uncertainty due to the hardware trigger efficiency correction.

The simulation PID response correction has two sources of uncertainty, one from the kernel density estimation and one from the finite size of the calibration samples. The width of the kernel is increased by 50% and the variation in the efficiency ratios is assigned as the systematic uncertainty. For the finite size of the PID calibration sample, a bootstrapping method [29] finds a change of less than 0.02% in the efficiency ratios which is thus neglected.

Systematic uncertainties due to the mass fit model are estimated by using alternative signal and background probability density functions (PDFs). There are two alternative $\Sigma_c^{(*)++}$ Breit-Wigner PDFs: either the Blatt-Weiskopf form factor barrier radius [30], d, is doubled, or the $\Sigma_c^{(*)++}$ mass and width are floated while the $m_{\Sigma_c^{*++}} - m_{\Sigma_c^{++}}$ mass difference is fixed. The two alternative peaking Λ_b^0 PDFs are either the fixed tail parameters are varied by $\pm 1\sigma$ of their simulation fit uncertainties or a Hypatia function [31] is used instead of the two Crystal Ball functions. The alternative background parametrization in $m_{\Lambda_b^0}$ uses a second-order Chebychev polynomial instead of the default exponential function. For the threshold function background PDFs in $m_{\Lambda_c^+ \pi^+}$, an additional quadratic term is multiplied to the default threshold function as an alternative PDF. The six alternative PDFs are used one-at-a-time and two-at-a-time as alternative models to fit data, where the latter accounts for the correlation between alternative PDFs. The largest difference in fitted yields between any two models, default or alternative, is taken as the systematic uncertainty on the fitted yields. These uncertainties are subsequently propagated to the ratio of branching fractions by accounting for the correlation between different decay modes.

When calculating the default efficiencies, the kinematic distributions of the simulated Λ_b^0 particles are corrected in bins of η and $p_{\rm T}$ to better match those in data using $\Lambda_b^0 \to \Lambda_c^+ \bar{D}^0 K^-$ decays. The systematic uncertainty of this correction is estimated by using an alternative (narrower) binning scheme. A systematic uncertainty of 0.05% is estimated for the ratio of branching fractions $\mathcal{B}(\Lambda_b^0 \to \Sigma_c^{++} D^- K^-)/\mathcal{B}(\Lambda_b^0 \to \Lambda_c^+ \bar{D}^0 K^-)$ and is negligible for the ratios of branching fractions between signal modes.

The systematic uncertainty due to the limited size of the simulated signal and reference modes is estimated by assuming that the efficiencies follow a binomial distribution. The systematic uncertainty due to multiple candidate removal is calculated by assuming all removed candidates would increase the signal or reference mode yields by the number of candidates removed. The ratios of branching fractions are recalculated with the increased yields, and the differences are assigned as a systematic uncertainty.

Although the simulated decay $\Lambda_c^+ \to p K^- \pi^+$ includes intermediate resonances, its simulated Dalitz distribution does not perfectly match that of real data. The Λ_c^+ Dalitz distribution correction is estimated from $\Lambda_b^0 \to \Lambda_c^+ \bar{D}^0 K^-$ decays by comparing the Λ_c^+ Dalitz distribution in data to simulation. This correction is then applied to the simulated signal decay modes, and the differences in the ratios of branching fractions are taken as systematic uncertainties.

TABLE I. Summary of systematic uncertainties. The correlation between those due to the limited statistics of simulated samples and other sources is considered. Systematics uncertainties due to the modeling of track reconstruction and trigger efficiencies are assumed to cancel out in the ratios between signal modes.

Source	$\frac{\mathcal{B}(\Lambda_b^0\to\Sigma_c^{++}D^-K^-)}{\mathcal{B}(\Lambda_b^0\to\Lambda_c^+\bar{D}^0K^-)}$ (%)	$\frac{\mathcal{B}(\Lambda_b^0\to\Sigma_c^{*++}D^-K^-)}{\mathcal{B}(\Lambda_b^0\to\Sigma_c^{++}D^-K^-)}$ (%)	$\frac{\mathcal{B}(\Lambda_b^0\to\Sigma_c^{++}D^{*-}K^-)}{\mathcal{B}(\Lambda_b^0\to\Sigma_c^{++}D^-K^-)}$ (%)	$\frac{\mathcal{B}(\Lambda_b^0\to\Sigma_c^{*++}D^{*-}K^-)}{\mathcal{B}(\Lambda_b^0\to\Sigma_c^{++}D^-K^-)}$ (%)
Track reconstruction	3.22	...	...	...
Trigger efficiency	0.77	...	...	...
PID correction algorithm	0.20	0.05	0.06	0.28
Fitting model	1.36	3.67	2.00	1.29
Kinematic reweight	0.05	< 0.01	< 0.01	< 0.01
Statistics of simulated samples	2.71	4.01	3.59	5.58
NDC backgrounds	1.66	2.44	0.71	2.10
Modeling of Λ_c^+ decay amplitude	1.28	0.09	1.58	0.41
Multiple candidates	0.06	1.51	0.38	3.44
Total	5.64	6.21	5.70	7.35

The contamination by NDC decays of Λ_b^0 candidates can be estimated by fitting the $m_{\Lambda_b^0}$ distribution in the sideband regions of $m_{pK^-\pi^+}$ and $m_{K^+\pi^-}$ ($m_{K^+\pi^-\pi^-}$), then extrapolating the yields of NDC Λ_b^0 to the Λ_c^+ and D^- (or D^{*-}) signal window. This procedure estimates an NDC contamination of 0.9% for $\Lambda_b^0\to\Sigma_c^{++}D^-K^-$, 4.8% for $\Lambda_b^0\to\Sigma_c^{*++}D^-K^-$, 1.1% for $\Lambda_b^0\to\Sigma_c^{(*)++}D^{*-}K^-$, 4.1% for $\Lambda_b^0\to\Sigma_c^{*++}D^{*-}K^-$ and 3.2% for $\Lambda_b^0\to\Lambda_c^+\bar{D}^0K^-$. However, the Λ_c^+ and D^- (or D^{*-}) mass constraints smear the $m_{\Lambda_b^0}$ mass peaks of NDC backgrounds reducing the potential bias that NDC backgrounds would have on the yields of doubly charmed decay modes. As a conservative estimate, half of the NDC contamination rate is taken as a systematic uncertainty on the fitted yields, which is then propagated to the ratios of branching fractions.

A summary of the systematic uncertainties is shown in Table I, and the systematic uncertainty for each ratio is calculated by considering the correlations between statistical limitations of simulated samples and kinematic reweighting or Λ_c^+ decay amplitude modeling, utilizing a correlation matrix with nondiagonal elements set to 1 for these sources.

Significance of signal modes. To determine the statistical significance of the signal modes, two methods are employed. For the Σ_c^{++} modes, $\Lambda_b^0\to\Sigma_c^{++}D^-K^-$ and $\Lambda_b^0\to\Sigma_c^{++}D^{*-}K^-$, the statistical significances are estimated via Wilks' theorem [32], which relies on the log-likelihood difference, $\Delta\mathcal{L}$, between the default fit and a fit without the Σ_c^{++} signal mode. Under the null (no Σ_c^{++} signal) hypothesis, Wilks' theorem specifies that the value of $2\Delta\mathcal{L}$ follows a χ^2 distribution, with a number of degrees-of-freedom equal to the number of additional floating parameters in the default fit. The p values calculated reject the null hypothesis at significances of 32σ for $\Lambda_b^0\to\Sigma_c^{++}D^-K^-$ and 21σ for $\Lambda_b^0\to\Sigma_c^{++}D^{*-}K^-$. Because these are well above the 5σ observation threshold, the effects of systematic uncertainties are not considered.

For the Σ_c^{*++} modes, pseudoexperiments are used to determine the significances of the $\Lambda_b^0\to\Sigma_c^{*++}D^-K^-$ and $\Lambda_b^0\to\Sigma_c^{*++}D^{*-}K^-$ signal modes. The pseudoexperiments are generated from the mass fit model which gives the lowest yield of $\Lambda_b^0\to\Sigma_c^{*++}D^-K^-$ ($\Lambda_b^0\to\Sigma_c^{*++}D^{*-}K^-$). This lowest yield model can be the default model or one of the alternative models, which incorporates systematic uncertainties into the calculation of statistical significance. The lowest yield model is used to generate 5000 pseudoexperiments with the yields of Σ_c^{*++} signal mode set to zero. Each pseudoexperiment is then fitted twice, once with the Σ_c^{*++} signal mode yield floating to determine the signal hypothesis log-likelihood, $\mathcal{L}_{\Sigma_c^{*++}}$, and once without the aforementioned signal component to determine the null hypothesis log-likelihood $\mathcal{L}_0$. The $-2\Delta\mathcal{L}=-2\times(\mathcal{L}_0-\mathcal{L}_{\Sigma_c^{*++}})$ distribution is then modeled as a χ^2 distribution. Subsequently, the upper tail of this distribution is extrapolated to the data $-2\Delta\mathcal{L}$ value to estimate a p value, which rejects the null hypotheses at significances of 13σ for $\Lambda_b^0\to\Sigma_c^{*++}D^-K^-$ and 9σ for $\Lambda_b^0\to\Sigma_c^{*++}D^{*-}K^-$.

Conclusion. The decays $\Lambda_b^0\to\Sigma_c^{++}D^-K^-$, $\Lambda_b^0\to\Sigma_c^{++}D^{*-}K^-$, $\Lambda_b^0\to\Sigma_c^{*++}D^-K^-$, and $\Lambda_b^0\to\Sigma_c^{*++}D^{*-}K^-$ have been observed for the first time by employing the LHCb data sample collected during the Run 2 data-taking period, corresponding to an integrated luminosity of 6 fb^{-1}. Their measured relative branching fractions are

$$\frac{\mathcal{B}(\Lambda_b^0 \to \Sigma_c^{++} D^- K^-)}{\mathcal{B}(\Lambda_b^0 \to \Lambda_c^+ \bar{D}^0 K^-)} = 0.282 \pm 0.016 \pm 0.016 \pm 0.005,$$

$$\frac{\mathcal{B}(\Lambda_b^0 \to \Sigma_c^{*++} D^- K^-)}{\mathcal{B}(\Lambda_b^0 \to \Sigma_c^{++} D^- K^-)} = 0.460 \pm 0.052 \pm 0.028,$$

$$\frac{\mathcal{B}(\Lambda_b^0 \to \Sigma_c^{++} D^{*-} K^-)}{\mathcal{B}(\Lambda_b^0 \to \Sigma_c^{++} D^- K^-)} = 2.261 \pm 0.202 \pm 0.129 \pm 0.046,$$

$$\frac{\mathcal{B}(\Lambda_b^0 \to \Sigma_c^{*++} D^{*-} K^-)}{\mathcal{B}(\Lambda_b^0 \to \Sigma_c^{++} D^- K^-)} = 0.896 \pm 0.137 \pm 0.066 \pm 0.018,$$

where the first uncertainties are statistical, the second are systematic, and the third are due to uncertainties in the branching fractions of intermediate particle decays. These results provide important inputs for theoretical studies of pentaquark production, in particular in terms of the molecular picture.

These four decay modes only have $\mathcal{O}(100)$ candidates each in the LHCb Run 2 dataset, which is statistically insufficient to perform an amplitude analysis. This limitation will be overcome with Run 3 data which is expected to increase the statistics by a large factor thanks to the increase in luminosity and trigger efficiency [33,34]. A future amplitude analysis of these four decay modes will help constrain the characteristics of the three observed pentaquark candidates, which, so far, have only been observed in the discovery channel $\Lambda_b^0 \to J/\psi p K^-$.

Acknowledgments. We express our gratitude to our colleagues in the CERN accelerator departments for the excellent performance of the LHC. We thank the technical and administrative staff at the LHCb institutes. We acknowledge support from CERN and from the national agencies: CAPES, CNPq, FAPERJ and FINEP (Brazil); MOST and NSFC (China); CNRS/IN2P3 (France); BMBF, DFG and MPG (Germany); INFN (Italy); NWO (Netherlands); MNiSW and NCN (Poland); MCID/IFA (Romania); MICINN (Spain); SNSF and SER (Switzerland); NASU (Ukraine); STFC (United Kingdom); DOE NP and NSF (USA). We acknowledge the computing resources that are provided by CERN, IN2P3 (France), KIT and DESY (Germany), INFN (Italy), SURF (Netherlands), PIC (Spain), GridPP (United Kingdom), CSCS (Switzerland), IFIN-HH (Romania), CBPF (Brazil), and Polish WLCG (Poland). We are indebted to the communities behind the multiple open-source software packages on which we depend. Individual groups or members have received support from ARC and ARDC (Australia); Key Research Program of Frontier Sciences of CAS, CAS PIFI, CAS CCEPP, Fundamental Research Funds for the Central Universities, and Sci. & Tech. Program of Guangzhou (China); Minciencias (Colombia); EPLANET, Marie Skłodowska-Curie Actions, ERC and NextGenerationEU (European Union); A*MIDEX, ANR, IPhU and Labex P2IO, and Région Auvergne-Rhône-Alpes (France); AvH Foundation (Germany); ICSC (Italy); GVA, XuntaGal, GENCAT, Inditex, InTalent and Prog. Atracción Talento, CM (Spain); SRC (Sweden); the Leverhulme Trust, the Royal Society and UKRI (United Kingdom).

[1] M. Gell-Mann, A schematic model of baryons and mesons, Phys. Lett. **8**, 214 (1964); G. Zweig, An SU_3 model for strong interaction symmetry and its breaking; Version 1, Report No. CERN-TH-401, CERN, Geneva, 1964.
[2] M. R. Pennington, Evolving images of the proton: Hadron physics over the past 40 years, J. Phys. G **43**, 054001 (2016).
[3] M. Amaryan, History and geography of light pentaquark searches: Challenges and pitfalls, Eur. Phys. J. Plus **137**, 684 (2022).
[4] G. C. Rossi and G. Veneziano, Tetra-quarks, penta-quarks and the like: Old and new views, Nucl. Part. Phys. Proc. **312–317**, 140 (2021).
[5] R. Aaij *et al.* (LHCb Collaboration), Observation of $J/\psi p$ resonances consistent with pentaquark states in $\Lambda_b^0 \to J/\psi p K^-$ decays, Phys. Rev. Lett. **115**, 072001 (2015).
[6] R. Aaij *et al.* (LHCb Collaboration), Model-independent evidence for $J/\psi p$ contributions to $\Lambda_b^0 \to J/\psi p K^-$ decays, Phys. Rev. Lett. **117**, 082002 (2016).
[7] R. Aaij *et al.* (LHCb Collaboration), Observation of a narrow pentaquark state, $P_c(4312)^+$, and of two-peak structure of the $P_c(4450)^+$, Phys. Rev. Lett. **122**, 222001 (2019).
[8] S. Weinberg, Evidence that the deuteron is not an elementary particle, Phys. Rev. **137**, B672 (1965).
[9] M.-L. Du, V. Baru, F.-K. Guo, C. Hanhart, U.-G. Meißner, J. A. Oller, and Q. Wang, Revisiting the nature of the P_c pentaquarks, J. High Energy Phys. 08 (2021) 157.
[10] T. J. Burns and E. S. Swanson, Experimental constraints on the properties of P_c states, Eur. Phys. J. A **58**, 68 (2022).
[11] J. He and D.-Y. Chen, Molecular states from $\Sigma_c^{(*)} \bar{D}^{(*)} - \Lambda_c \bar{D}^{(*)}$ interaction, Eur. Phys. J. C **79**, 887 (2019).
[12] Y.-W. Pan, M.-Z. Liu, and L.-S. Geng, Production rates of hidden-charm pentaquark molecules in Λ_b decays, Phys. Rev. D **108**, 114022 (2023).
[13] X.-H. Liu, Q. Wang, and Q. Zhao, Understanding the newly observed heavy pentaquark candidates, Phys. Lett. B **757**, 231 (2016).

[14] A. A. Alves, Jr. *et al.* (LHCb Collaboration), The LHCb detector at the LHC, J. Instrum. **3**, S08005 (2008).
[15] LHCb Collaboration, LHCb detector performance, Int. J. Mod. Phys. A **30**, 1530022 (2015).
[16] R. Aaij *et al.*, The LHCb trigger and its performance in 2011, J. Instrum. **8**, P04022 (2013).
[17] T. Likhomanenko, P. Ilten, E. Khairullin, A. Rogozhnikov, A. Ustyuzhanin, and M. Williams, LHCb topological trigger reoptimization, J. Phys. Conf. Ser. **664**, 082025 (2015).
[18] T. Sjöstrand, S. Mrenna, and P. Skands, A brief introduction to PYTHIA 8.1, Comput. Phys. Commun. **178**, 852 (2008); PYTHIA 6.4 physics and manual, J. High Energy Phys. 05 (2006) 026.
[19] I. Belyaev *et al.*, Handling of the generation of primary events in Gauss, the LHCb simulation framework, J. Phys. Conf. Ser. **331**, 032047 (2011).
[20] D. J. Lange, The EvtGen particle decay simulation package, Nucl. Instrum. Methods Phys. Res., Sect. A **462**, 152 (2001).
[21] N. Davidson, T. Przedzinski, and Z. Was, PHOTOS interface in C++: Technical and physics documentation, Comput. Phys. Commun. **199**, 86 (2016).
[22] J. Allison *et al.* (Geant4 Collaboration), Geant4 developments and applications, IEEE Trans. Nucl. Sci. **53**, 270 (2006); S. Agostinelli *et al.* (Geant4 Collaboration), Geant4: A simulation toolkit, Nucl. Instrum. Methods Phys. Res., Sect. A **506**, 250 (2003).
[23] M. Clemencic, G. Corti, S. Easo, C. R. Jones, S. Miglioranzi, M. Pappagallo, and P. Robbe, The LHCb simulation application, Gauss: Design, evolution and experience, J. Phys. Conf. Ser. **331**, 032023 (2011).
[24] A. Poluektov, Kernel density estimation of a multidimensional efficiency profile, J. Instrum. **10**, P02011 (2015).
[25] R. L. Workman *et al.* (Particle Data Group), Review of particle physics, Prog. Theor. Exp. Phys. **2022**, 083C01 (2022).
[26] T. Skwarnicki, A study of the radiative cascade transitions between the Upsilon-prime and Upsilon resonances, Ph.D. thesis, Institute of Nuclear Physics, Krakow, 1986.
[27] M. Pivk and F. R. Le Diberder, sPlot: A statistical tool to unfold data distributions, Nucl. Instrum. Methods Phys. Res., Sect. A **555**, 356 (2005).
[28] LHCb Collaboration, Measurement of the track reconstruction efficiency at LHCb, J. Instrum. **10**, P02007 (2015).
[29] L. Anderlini *et al.*, The PIDCalib package, Report No. LHCb-PUB-2016-021, 2016.
[30] J. M. Blatt and V. F. Weisskopf, *Theoretical Nuclear Physics* (Springer, New York, 1952).
[31] D. Martínez Santos and F. Dupertuis, Mass distributions marginalized over per-event errors, Nucl. Instrum. Methods Phys. Res., Sect. A **764**, 150 (2014).
[32] S. S. Wilks, The large-sample distribution of the likelihood ratio for testing composite hypotheses, Ann. Math. Stat. **9**, 60 (1938).
[33] LHCb Collaboration, Framework TDR for the LHCb upgrade: Technical design report, Report No. CERN-LHCC-2012-007, 2012.
[34] R. Aaij *et al.* (LHCb Collaboration), The LHCb upgrade I, J. Instrum. **19**, P05065 (2024).

R. Aaij,[35] A. S. W. Abdelmotteleb,[54] C. Abellan Beteta,[48] F. Abudinén,[54] T. Ackernley,[58] A. A. Adefisoye,[66] B. Adeva,[44] M. Adinolfi,[52] P. Adlarson,[79] C. Agapopoulou,[46] C. A. Aidala,[80] Z. Ajaltouni,[11] S. Akar,[63] K. Akiba,[35] P. Albicocco,[25] J. Albrecht,[17] F. Alessio,[46] M. Alexander,[57] Z. Aliouche,[60] P. Alvarez Cartelle,[53] R. Amalric,[15] S. Amato,[3] J. L. Amey,[52] Y. Amhis,[13,46] L. An,[6] L. Anderlini,[24] M. Andersson,[48] A. Andreianov,[41] P. Andreola,[48] M. Andreotti,[23] D. Andreou,[66] A. Anelli,[28,b] D. Ao,[7] F. Archilli,[34,c] M. Argenton,[23] S. Arguedas Cuendis,[9] A. Artamonov,[41] M. Artuso,[66] E. Aslanides,[12] M. Atzeni,[62] B. Audurier,[14] D. Bacher,[61] I. Bachiller Perea,[10] S. Bachmann,[19] M. Bachmayer,[47] J. J. Back,[54] P. Baladron Rodriguez,[44] V. Balagura,[14] W. Baldini,[23] J. Baptista de Souza Leite,[58] M. Barbetti,[24,d] I. R. Barbosa,[67] R. J. Barlow,[60] S. Barsuk,[13] W. Barter,[56] M. Bartolini,[53] J. Bartz,[66] F. Baryshnikov,[41] J. M. Basels,[16] G. Bassi,[32] B. Batsukh,[5] A. Battig,[17] A. Bay,[47] A. Beck,[54] M. Becker,[17] F. Bedeschi,[32] I. B. Bediaga,[2] A. Beiter,[66] S. Belin,[44] V. Bellee,[48] K. Belous,[41] I. Belov,[26] I. Belyaev,[33] G. Benane,[12] G. Bencivenni,[25] E. Ben-Haim,[15] A. Berezhnoy,[41] R. Bernet,[48] S. Bernet Andres,[42] C. Bertella,[60] A. Bertolin,[30] C. Betancourt,[48] F. Betti,[56] J. Bex,[53] Ia. Bezshyiko,[48] J. Bhom,[38] M. S. Bieker,[17] N. V. Biesuz,[23] P. Billoir,[15] A. Biolchini,[35] M. Birch,[59] F. C. R. Bishop,[10] A. Bitadze,[60] A. Bizzeti, T. Blake,[54] F. Blanc,[47] J. E. Blank,[17] S. Blusk,[66] V. Bocharnikov,[41] J. A. Boelhauve,[17] O. Boente Garcia,[14] T. Boettcher,[63] A. Bohare,[56] A. Boldyrev,[41] C. S. Bolognani,[76] R. Bolzonella,[23,e] N. Bondar,[41] F. Borgato,[30,46,f] S. Borghi,[60] M. Borsato,[28,b] J. T. Borsuk,[38] S. A. Bouchiba,[47] T. J. V. Bowcock,[58] A. Boyer,[46] C. Bozzi,[23] M. J. Bradley,[59] A. Brea Rodriguez,[44] N. Breer,[17] J. Brodzicka,[38] A. Brossa Gonzalo,[44] J. Brown,[58] D. Brundu,[29] E. Buchanan,[56] A. Buonaura,[48] L. Buonincontri,[30,f] A. T. Burke,[60] C. Burr,[46] A. Bursche,[69] A. Butkevich,[41] J. S. Butter,[53] J. Buytaert,[46] W. Byczynski,[46] S. Cadeddu,[29] H. Cai,[71] R. Calabrese,[23,e] L. Calefice,[43] S. Cali,[25] M. Calvi,[28,b] M. Calvo Gomez,[42] J. I. Cambon Bouzas,[44] P. Campana,[25] D. H. Campora Perez,[76] A. F. Campoverde Quezada,[7]

S. Capelli,[28,b] L. Capriotti,[23] R. Caravaca-Mora,[9] A. Carbone,[22,g] L. Carcedo Salgado,[44] R. Cardinale,[26,h] A. Cardini,[29] P. Carniti,[28,b] L. Carus,[19] A. Casais Vidal,[62] R. Caspary,[19] G. Casse,[58] J. Castro Godinez,[9] M. Cattaneo,[46] G. Cavallero,[23] V. Cavallini,[23,e] S. Celani,[19] J. Cerasoli,[12] D. Cervenkov,[61] S. Cesare,[27,i] A. J. Chadwick,[58] I. Chahrour,[80] M. Charles,[15] Ph. Charpentier,[46] C. A. Chavez Barajas,[58] M. Chefdeville,[10] C. Chen,[12] S. Chen,[5] Z. Chen,[7] A. Chernov,[38] S. Chernyshenko,[50] V. Chobanova,[78] S. Cholak,[47] M. Chrzaszcz,[38] A. Chubykin,[41] V. Chulikov,[41] P. Ciambrone,[25] X. Cid Vidal,[44] G. Ciezarek,[46] P. Cifra,[46] P. E. L. Clarke,[56] M. Clemencic,[46] H. V. Cliff,[53] J. Closier,[46] C. Cocha Toapaxi,[19] V. Coco,[46] J. Cogan,[12] E. Cogneras,[11] L. Cojocariu,[40] P. Collins,[46] T. Colombo,[46] A. Comerma-Montells,[43] L. Congedo,[21] A. Contu,[29] N. Cooke,[57] I. Corredoira,[44] A. Correia,[15] G. Corti,[46] J. J. Cottee Meldrum,[52] B. Couturier,[46] D. C. Craik,[48] M. Cruz Torres,[2,j] E. Curras Rivera,[47] R. Currie,[56] C. L. Da Silva,[65] S. Dadabaev,[41] L. Dai,[68] X. Dai,[6] E. Dall'Occo,[17] J. Dalseno,[44] C. D'Ambrosio,[46] J. Daniel,[11] A. Danilina,[41] P. d'Argent,[21] A. Davidson,[54] J. E. Davies,[60] A. Davis,[60] O. De Aguiar Francisco,[60] C. De Angelis,[29,k] F. De Benedetti,[46] J. de Boer,[35] K. De Bruyn,[75] S. De Capua,[60] M. De Cian,[19,46] U. De Freitas Carneiro Da Graca,[2,l] E. De Lucia,[25] J. M. De Miranda,[2] L. De Paula,[3] M. De Serio,[21,m] D. De Simone,[48] P. De Simone,[25] F. De Vellis,[17] J. A. de Vries,[76] F. Debernardis,[21] D. Decamp,[10] V. Dedu,[12] L. Del Buono,[15] B. Delaney,[62] H.-P. Dembinski,[17] J. Deng,[8] V. Denysenko,[48] O. Deschamps,[11] F. Dettori,[29,k] B. Dey,[74] P. Di Nezza,[25] I. Diachkov,[41] S. Didenko,[41] S. Ding,[66] L. Dittmann,[19] V. Dobishuk,[50] A. D. Docheva,[57] A. Dolmatov,[41] C. Dong,[4] A. M. Donohoe,[20] F. Dordei,[29] A. C. dos Reis,[2] A. D. Dowling,[66] A. G. Downes,[10] W. Duan,[69] P. Duda,[77] M. W. Dudek,[38] L. Dufour,[46] V. Duk,[31] P. Durante,[46] M. M. Duras,[77] J. M. Durham,[65] O. D. Durmus,[74] A. Dziurda,[38] A. Dzyuba,[41] S. Easo,[55] E. Eckstein,[73] U. Egede,[1] A. Egorychev,[41] V. Egorychev,[41] S. Eisenhardt,[56] E. Ejopu,[60] S. Ek-In,[47] L. Eklund,[79] M. Elashri,[63] J. Ellbracht,[17] S. Ely,[59] A. Ene,[40] E. Epple,[63] S. Escher,[16] J. Eschle,[48] S. Esen,[19] T. Evans,[60] F. Fabiano,[29,46,k] L. N. Falcao,[2] Y. Fan,[7] B. Fang,[71,13] L. Fantini,[31,n] M. Faria,[47] K. Farmer,[56] D. Fazzini,[28,b] L. Felkowski,[77] M. Feng,[5,7] M. Feo,[46] M. Fernandez Gomez,[44] A. D. Fernez,[64] F. Ferrari,[22] F. Ferreira Rodrigues,[3] S. Ferreres Sole,[35] M. Ferrillo,[48] M. Ferro-Luzzi,[46] S. Filippov,[41] R. A. Fini,[21] M. Fiorini,[23,e] K. M. Fischer,[61] D. S. Fitzgerald,[80] C. Fitzpatrick,[60] F. Fleuret,[14] M. Fontana,[22] L. F. Foreman,[60] R. Forty,[46] D. Foulds-Holt,[53] M. Franco Sevilla,[64] M. Frank,[46] E. Franzoso,[23,e] G. Frau,[19] C. Frei,[46] D. A. Friday,[60] J. Fu,[7] Q. Fuehring,[17] Y. Fujii,[1] T. Fulghesu,[15] E. Gabriel,[35] G. Galati,[21,m] M. D. Galati,[35] A. Gallas Torreira,[44] D. Galli,[22,g] S. Gambetta,[56] M. Gandelman,[3] P. Gandini,[27] H. Gao,[7] R. Gao,[61] Y. Gao,[8] Y. Gao,[6] Y. Gao,[8] M. Garau,[29,k] L. M. Garcia Martin,[47] P. Garcia Moreno,[43] J. García Pardiñas,[46] K. G. Garg,[8] L. Garrido,[43] C. Gaspar,[46] R. E. Geertsema,[35] L. L. Gerken,[17] E. Gersabeck,[60] M. Gersabeck,[60] T. Gershon,[54] Z. Ghorbanimoghaddam,[52] L. Giambastiani,[30,f] F. I. Giasemis,[15,o] V. Gibson,[53] H. K. Giemza,[39] A. L. Gilman,[61] M. Giovannetti,[25] A. Gioventù,[43] P. Gironella Gironell,[43] C. Giugliano,[23,e] M. A. Giza,[38] E. L. Gkougkousis,[59] F. C. Glaser,[13,19] V. V. Gligorov,[15] C. Göbel,[67] E. Golobardes,[42] D. Golubkov,[41] A. Golutvin,[59,41,46] A. Gomes,[2,a,p] S. Gomez Fernandez,[43] F. Goncalves Abrantes,[61] M. Goncerz,[38] G. Gong,[4] J. A. Gooding,[17] I. V. Gorelov,[41] C. Gotti,[28] J. P. Grabowski,[73] L. A. Granado Cardoso,[46] E. Graugés,[43] E. Graverini,[47,q] L. Grazette,[54] G. Graziani, A. T. Grecu,[40] L. M. Greeven,[35] N. A. Grieser,[63] L. Grillo,[57] S. Gromov,[41] C. Gu,[14] M. Guarise,[23] M. Guittiere,[13] V. Guliaeva,[41] P. A. Günther,[19] A.-K. Guseinov,[47] E. Gushchin,[41] Y. Guz,[6,41,46] T. Gys,[46] K. Habermann,[73] T. Hadavizadeh,[1] C. Hadjivasiliou,[64] G. Haefeli,[47] C. Haen,[46] J. Haimberger,[46] M. Hajheidari,[46] M. M. Halvorsen,[46] P. M. Hamilton,[64] J. Hammerich,[58] Q. Han,[8] X. Han,[19] S. Hansmann-Menzemer,[19] L. Hao,[7] N. Harnew,[61] T. Harrison,[58] M. Hartmann,[13] J. He,[7,r] K. Heijhoff,[35] F. Hemmer,[46] C. Henderson,[63] R. D. L. Henderson,[1,54] A. M. Hennequin,[46] K. Hennessy,[58] L. Henry,[47] J. Herd,[59] P. Herrero Gascon,[19] J. Heuel,[16] A. Hicheur,[3] G. Hijano Mendizabal,[48] D. Hill,[47] S. E. Hollitt,[17] J. Horswill,[60] R. Hou,[8] Y. Hou,[10] N. Howarth,[58] J. Hu,[19] J. Hu,[69] W. Hu,[6] X. Hu,[4] W. Huang,[7] W. Hulsbergen,[35] R. J. Hunter,[54] M. Hushchyn,[41] D. Hutchcroft,[58] D. Ilin,[41] P. Ilten,[63] A. Inglessi,[41] A. Iniukhin,[41] A. Ishteev,[41] K. Ivshin,[41] R. Jacobsson,[46] H. Jage,[16] S. J. Jaimes Elles,[45,72] S. Jakobsen,[46] E. Jans,[35] B. K. Jashal,[45] A. Jawahery,[64,46] V. Jevtic,[17] E. Jiang,[64] X. Jiang,[5,7] Y. Jiang,[7] Y. J. Jiang,[6] M. John,[61] D. Johnson,[51] C. R. Jones,[53] T. P. Jones,[54] S. Joshi,[39] B. Jost,[46] N. Jurik,[46] I. Juszczak,[38] D. Kaminaris,[47] S. Kandybei,[49] Y. Kang,[4] M. Karacson,[46] D. Karpenkov,[41] A. Kauniskangas,[47] J. W. Kautz,[63] F. Keizer,[46] M. Kenzie,[53] T. Ketel,[35] B. Khanji,[66]

A. Kharisova,[41] S. Kholodenko,[32] G. Khreich,[13] T. Kirn,[16] V. S. Kirsebom,[28,b] O. Kitouni,[62] S. Klaver,[36] N. Kleijne,[32,s] K. Klimaszewski,[39] M. R. Kmiec,[39] S. Koliiev,[50] L. Kolk,[17] A. Konoplyannikov,[41] P. Kopciewicz,[37,46] P. Koppenburg,[35] M. Korolev,[41] I. Kostiuk,[35] O. Kot,[50] S. Kotriakhova, A. Kozachuk,[41] P. Kravchenko,[41] L. Kravchuk,[41] M. Kreps,[54] S. Kretzschmar,[16] P. Krokovny,[41] W. Krupa,[66] W. Krzemien,[39] J. Kubat,[19] S. Kubis,[77] W. Kucewicz,[38] M. Kucharczyk,[38] V. Kudryavtsev,[41] E. Kulikova,[41] A. Kupsc,[79] B. K. Kutsenko,[12] D. Lacarrere,[46] A. Lai,[29] A. Lampis,[29] D. Lancierini,[53] C. Landesa Gomez,[44] J. J. Lane,[1] R. Lane,[52] C. Langenbruch,[19] J. Langer,[17] O. Lantwin,[41] T. Latham,[54] F. Lazzari,[32,q] C. Lazzeroni,[51] R. Le Gac,[12] R. Lefèvre,[11] A. Leflat,[41] S. Legotin,[41] M. Lehuraux,[54] E. Lemos Cid,[46] O. Leroy,[12] T. Lesiak,[38] B. Leverington,[19] A. Li,[4] H. Li,[69] K. Li,[8] L. Li,[60] P. Li,[46] P.-R. Li,[70] S. Li,[8] T. Li,[5,t] T. Li,[69] Y. Li,[8] Y. Li,[5] Z. Li,[66] Z. Lian,[4] X. Liang,[66] S. Libralon,[45] C. Lin,[7] T. Lin,[55] R. Lindner,[46] V. Lisovskyi,[47] R. Litvinov,[29,k] F. L. Liu,[1] G. Liu,[69] K. Liu,[70] Q. Liu,[7] S. Liu,[5,7] Y. Liu,[56] Y. Liu,[70] Y. L. Liu,[59] A. Lobo Salvia,[43] A. Loi,[29] J. Lomba Castro,[44] T. Long,[53] J. H. Lopes,[3] A. Lopez Huertas,[43] S. López Soliño,[44] G. H. Lovell,[53] C. Lucarelli,[24,d] D. Lucchesi,[30,f] S. Luchuk,[41] M. Lucio Martinez,[76] V. Lukashenko,[35,50] Y. Luo,[6] A. Lupato,[30] E. Luppi,[23,e] K. Lynch,[20] X.-R. Lyu,[7] G. M. Ma,[4] R. Ma,[7] S. Maccolini,[17] F. Machefert,[13] F. Maciuc,[40] B. M. Mack,[66] I. Mackay,[61] L. M. Mackey,[66] L. R. Madhan Mohan,[53] M. M. Madurai,[51] A. Maevskiy,[41] D. Magdalinski,[35] D. Maisuzenko,[41] M. W. Majewski,[37] J. J. Malczewski,[38] S. Malde,[61] B. Malecki,[38,46] L. Malentacca,[46] A. Malinin,[41] T. Maltsev,[41] G. Manca,[29,k] G. Mancinelli,[12] C. Mancuso,[27,13,i] R. Manera Escalero,[43] D. Manuzzi,[22] D. Marangotto,[27,i] J. F. Marchand,[10] R. Marchevski,[47] U. Marconi,[22] S. Mariani,[46] C. Marin Benito,[43] J. Marks,[19] A. M. Marshall,[52] P. J. Marshall,[58] G. Martelli,[31,n] G. Martellotti,[33] L. Martinazzoli,[46] M. Martinelli,[28,b] D. Martinez Santos,[44] F. Martinez Vidal,[45] A. Massafferri,[2] M. Materok,[16] R. Matev,[46] A. Mathad,[46] V. Matiunin,[41] C. Matteuzzi,[66] K. R. Mattioli,[14] A. Mauri,[59] E. Maurice,[14] J. Mauricio,[43] P. Mayencourt,[47] M. Mazurek,[39] M. McCann,[59] L. Mcconnell,[20] T. H. McGrath,[60] N. T. McHugh,[57] A. McNab,[60] R. McNulty,[20] B. Meadows,[63] G. Meier,[17] D. Melnychuk,[39] M. Merk,[35,76] A. Merli,[27,i] L. Meyer Garcia,[3] D. Miao,[5,7] H. Miao,[7] M. Mikhasenko,[73,u] D. A. Milanes,[72] A. Minotti,[28,b] E. Minucci,[66] T. Miralles,[11] B. Mitreska,[17] D. S. Mitzel,[17] A. Modak,[55] A. Mödden,[17] R. A. Mohammed,[61] R. D. Moise,[16] S. Mokhnenko,[41] T. Mombächer,[46] M. Monk,[54,1] S. Monteil,[11] A. Morcillo Gomez,[44] G. Morello,[25] M. J. Morello,[32,s] M. P. Morgenthaler,[19] A. B. Morris,[46] A. G. Morris,[12] R. Mountain,[66] H. Mu,[4] Z. M. Mu,[6] E. Muhammad,[54] F. Muheim,[56] M. Mulder,[75] K. Müller,[48] F. Muñoz-Rojas,[9] R. Murta,[59] P. Naik,[58] T. Nakada,[47] R. Nandakumar,[55] T. Nanut,[46] I. Nasteva,[3] M. Needham,[56] N. Neri,[27,i] S. Neubert,[73] N. Neufeld,[46] P. Neustroev,[41] J. Nicolini,[17,13] D. Nicotra,[76] E. M. Niel,[47] N. Nikitin,[41] P. Nogga,[73] N. S. Nolte,[62] C. Normand,[52] J. Novoa Fernandez,[44] G. Nowak,[63] C. Nunez,[80] H. N. Nur,[57] A. Oblakowska-Mucha,[37] V. Obraztsov,[41] T. Oeser,[16] S. Okamura,[23,46,e] A. Okhotnikov,[41] R. Oldeman,[29,k] F. Oliva,[56] M. Olocco,[17] C. J. G. Onderwater,[76] R. H. O'Neil,[56] J. M. Otalora Goicochea,[3] P. Owen,[48] A. Oyanguren,[45] O. Ozcelik,[56] K. O. Padeken,[73] B. Pagare,[54] P. R. Pais,[19] T. Pajero,[61] A. Palano,[21] M. Palutan,[25] G. Panshin,[41] L. Paolucci,[54] A. Papanestis,[55] M. Pappagallo,[21,m] L. L. Pappalardo,[23,e] C. Pappenheimer,[63] C. Parkes,[60] B. Passalacqua,[23] G. Passaleva,[24] D. Passaro,[32,s] A. Pastore,[21] M. Patel,[59] J. Patoc,[61] C. Patrignani,[22,g] C. J. Pawley,[76] A. Pellegrino,[35] M. Pepe Altarelli,[25] S. Perazzini,[22] D. Pereima,[41] A. Pereiro Castro,[44] P. Perret,[11] A. Perro,[46] K. Petridis,[52] A. Petrolini,[26,h] S. Petrucci,[56] J. P. Pfaller,[63] H. Pham,[66] L. Pica,[32,s] M. Piccini,[31] B. Pietrzyk,[10] G. Pietrzyk,[13] D. Pinci,[33] F. Pisani,[46] M. Pizzichemi,[28,b] V. Placinta,[40] M. Plo Casasus,[44] F. Polci,[15,46] M. Poli Lener,[25] A. Poluektov,[12] N. Polukhina,[41] I. Polyakov,[46] E. Polycarpo,[3] S. Ponce,[46] D. Popov,[7] S. Poslavskii,[41] K. Prasanth,[38] C. Prouve,[44] V. Pugatch,[50] G. Punzi,[32,q] W. Qian,[7] N. Qin,[4] S. Qu,[4] R. Quagliani,[47] R. I. Rabadan Trejo,[54] J. H. Rademacker,[52] M. Rama,[32] M. Ramírez García,[80] M. Ramos Pernas,[54] M. S. Rangel,[3] F. Ratnikov,[41] G. Raven,[36] M. Rebollo De Miguel,[45] F. Redi,[27,v] J. Reich,[52] F. Reiss,[60] Z. Ren,[7] P. K. Resmi,[61] R. Ribatti,[32,s] G. R. Ricart,[14,81] D. Riccardi,[32,s] S. Ricciardi,[55] K. Richardson,[62] M. Richardson-Slipper,[56] K. Rinnert,[58] P. Robbe,[13] G. Robertson,[57] E. Rodrigues,[58] E. Rodriguez Fernandez,[44] J. A. Rodriguez Lopez,[72] E. Rodriguez Rodriguez,[44] A. Rogovskiy,[55] D. L. Rolf,[46] P. Roloff,[46] V. Romanovskiy,[41] M. Romero Lamas,[44] A. Romero Vidal,[44] G. Romolini,[23] F. Ronchetti,[47] M. Rotondo,[25] S. R. Roy,[19] M. S. Rudolph,[66] T. Ruf,[46] M. Ruiz Diaz,[19] R. A. Ruiz Fernandez,[44] J. Ruiz Vidal,[79,w] A. Ryzhikov,[41] J. Ryzka,[37] J. J. Saavedra-Arias,[9] J. J. Saborido Silva,[44] R. Sadek,[14]

N. Sagidova,[41] D. Sahoo,[74] N. Sahoo,[51] B. Saitta,[29,k] M. Salomoni,[28,b] C. Sanchez Gras,[35] I. Sanderswood,[45] R. Santacesaria,[33] C. Santamarina Rios,[44] M. Santimaria,[25] L. Santoro,[2] E. Santovetti,[34] A. Saputi,[23,46] D. Saranin,[41] G. Sarpis,[56] M. Sarpis,[73] A. Sarti,[33] C. Satriano,[33,x] A. Satta,[34] M. Saur,[6] D. Savrina,[41] H. Sazak,[16] L. G. Scantlebury Smead,[61] A. Scarabotto,[17] S. Schael,[16] S. Scherl,[58] A. M. Schertz,[74] M. Schiller,[57] H. Schindler,[46] M. Schmelling,[18] B. Schmidt,[46] S. Schmitt,[16] H. Schmitz,[73] O. Schneider,[47] A. Schopper,[46] N. Schulte,[17] S. Schulte,[47] M. H. Schune,[13] R. Schwemmer,[46] G. Schwering,[16] B. Sciascia,[25] A. Sciuccati,[46] S. Sellam,[44] A. Semennikov,[41] T. Senger,[48] M. Senghi Soares,[36] A. Sergi,[26] N. Serra,[48] L. Sestini,[30] A. Seuthe,[17] Y. Shang,[6] D. M. Shangase,[80] M. Shapkin,[41] R. S. Sharma,[66] I. Shchemerov,[41] L. Shchutska,[47] T. Shears,[58] L. Shekhtman,[41] Z. Shen,[6] S. Sheng,[5,7] V. Shevchenko,[41] B. Shi,[7] E. B. Shields,[28,b] Y. Shimizu,[13] E. Shmanin,[41] R. Shorkin,[41] J. D. Shupperd,[66] R. Silva Coutinho,[66] G. Simi,[30,f] S. Simone,[21,m] N. Skidmore,[54] T. Skwarnicki,[66] M. W. Slater,[51] J. C. Smallwood,[61] E. Smith,[62] K. Smith,[65] M. Smith,[59] A. Snoch,[35] L. Soares Lavra,[56] M. D. Sokoloff,[63] F. J. P. Soler,[57] A. Solomin,[41,52] A. Solovev,[41] I. Solovyev,[41] R. Song,[1] Y. Song,[47] Y. Song,[4] Y. S. Song,[6] F. L. Souza De Almeida,[66] B. Souza De Paula,[3] E. Spadaro Norella,[27,i] E. Spedicato,[22] J. G. Speer,[17] E. Spiridenkov,[41] P. Spradlin,[57] V. Sriskaran,[46] F. Stagni,[46] M. Stahl,[46] S. Stahl,[46] S. Stanislaus,[61] E. N. Stein,[46] O. Steinkamp,[48] O. Stenyakin,[41] H. Stevens,[17] D. Strekalina,[41] Y. Su,[7] F. Suljik,[61] J. Sun,[29] L. Sun,[71] Y. Sun,[64] W. Sutcliffe,[48] P. N. Swallow,[51] F. Swystun,[53] A. Szabelski,[39] T. Szumlak,[37] Y. Tan,[4] S. Taneja,[60] M. D. Tat,[61] A. Terentev,[48] F. Terzuoli,[32,y] F. Teubert,[46] E. Thomas,[46] D. J. D. Thompson,[51] H. Tilquin,[59] V. Tisserand,[11] S. T'Jampens,[10] M. Tobin,[5] L. Tomassetti,[23,e] G. Tonani,[27,46,i] X. Tong,[6] D. Torres Machado,[2] L. Toscano,[17] D. Y. Tou,[4] C. Trippl,[42] G. Tuci,[19] N. Tuning,[35] L. H. Uecker,[19] A. Ukleja,[37] D. J. Unverzagt,[19] E. Ursov,[41] A. Usachov,[36] A. Ustyuzhanin,[41] U. Uwer,[19] V. Vagnoni,[22] A. Valassi,[46] G. Valenti,[22] N. Valls Canudas,[42] H. Van Hecke,[65] E. van Herwijnen,[59] C. B. Van Hulse,[44,z] R. Van Laak,[47] M. van Veghel,[35] R. Vazquez Gomez,[43] P. Vazquez Regueiro,[44] C. Vázquez Sierra,[44] S. Vecchi,[23] J. J. Velthuis,[52] M. Veltri,[24,aa] A. Venkateswaran,[47] M. Vesterinen,[54] M. Vieites Diaz,[46] X. Vilasis-Cardona,[42] E. Vilella Figueras,[58] A. Villa,[22] P. Vincent,[15] F. C. Volle,[13] D. vom Bruch,[12] V. Vorobyev,[41] N. Voropaev,[41] K. Vos,[76] G. Vouters,[10] C. Vrahas,[56] J. Wagner,[17] J. Walsh,[32] E. J. Walton,[1,54] G. Wan,[6] C. Wang,[19] G. Wang,[8] J. Wang,[6] J. Wang,[5] J. Wang,[4] J. Wang,[71] M. Wang,[27] N. W. Wang,[7] R. Wang,[52] X. Wang,[69] X. W. Wang,[59] Y. Wang,[8] Z. Wang,[13] Z. Wang,[4] Z. Wang,[27] J. A. Ward,[54,1] M. Waterlaat,[46] N. K. Watson,[51] D. Websdale,[59] Y. Wei,[6] B. D. C. Westhenry,[52] D. J. White,[60] M. Whitehead,[57] A. R. Wiederhold,[54] D. Wiedner,[17] G. Wilkinson,[61] M. K. Wilkinson,[63] M. Williams,[62] M. R. J. Williams,[56] R. Williams,[53] F. F. Wilson,[55] W. Wislicki,[39] M. Witek,[38] L. Witola,[19] C. P. Wong,[65] G. Wormser,[13] S. A. Wotton,[53] H. Wu,[66] J. Wu,[8] Y. Wu,[6] K. Wyllie,[46] S. Xian,[69] Z. Xiang,[5] Y. Xie,[8] A. Xu,[32] J. Xu,[7] L. Xu,[4] L. Xu,[4] M. Xu,[54] Z. Xu,[11] Z. Xu,[7] Z. Xu,[5] D. Yang,[4] S. Yang,[7] X. Yang,[6] Y. Yang,[26,h] Z. Yang,[6] Z. Yang,[64] V. Yeroshenko,[13] H. Yeung,[60] H. Yin,[8] C. Y. Yu,[6] J. Yu,[68] X. Yuan,[5] E. Zaffaroni,[47] M. Zavertyaev,[18] M. Zdybal,[38] M. Zeng,[4] C. Zhang,[6] D. Zhang,[8] J. Zhang,[7] L. Zhang,[4] S. Zhang,[68] S. Zhang,[6] Y. Zhang,[6] Y. Z. Zhang,[4] Y. Zhao,[19] A. Zharkova,[41] A. Zhelezov,[19] X. Z. Zheng,[4] Y. Zheng,[7] T. Zhou,[6] X. Zhou,[8] Y. Zhou,[7] V. Zhovkovska,[54] L. Z. Zhu,[7] X. Zhu,[4] X. Zhu,[8] V. Zhukov,[16] J. Zhuo,[45] Q. Zou,[5,7] D. Zuliani,[30,f] and G. Zunica[47]

(LHCb Collaboration)

[1]*School of Physics and Astronomy, Monash University, Melbourne, Australia*
[2]*Centro Brasileiro de Pesquisas Físicas (CBPF), Rio de Janeiro, Brazil*
[3]*Universidade Federal do Rio de Janeiro (UFRJ), Rio de Janeiro, Brazil*
[4]*Center for High Energy Physics, Tsinghua University, Beijing, China*
[5]*Institute Of High Energy Physics (IHEP), Beijing, China*
[6]*School of Physics State Key Laboratory of Nuclear Physics and Technology, Peking University, Beijing, China*
[7]*University of Chinese Academy of Sciences, Beijing, China*
[8]*Institute of Particle Physics, Central China Normal University, Wuhan, Hubei, China*
[9]*Consejo Nacional de Rectores (CONARE), San Jose, Costa Rica*
[10]*Université Savoie Mont Blanc, CNRS, IN2P3-LAPP, Annecy, France*

[11]*Université Clermont Auvergne, CNRS/IN2P3, LPC, Clermont-Ferrand, France*
[12]*Aix Marseille Univ, CNRS/IN2P3, CPPM, Marseille, France*
[13]*Université Paris-Saclay, CNRS/IN2P3, IJCLab, Orsay, France*
[14]*Laboratoire Leprince-Ringuet, CNRS/IN2P3, Ecole Polytechnique, Institut Polytechnique de Paris, Palaiseau, France*
[15]*LPNHE, Sorbonne Université, Paris Diderot Sorbonne Paris Cité, CNRS/IN2P3, Paris, France*
[16]*I. Physikalisches Institut, RWTH Aachen University, Aachen, Germany*
[17]*Fakultät Physik, Technische Universität Dortmund, Dortmund, Germany*
[18]*Max-Planck-Institut für Kernphysik (MPIK), Heidelberg, Germany*
[19]*Physikalisches Institut, Ruprecht-Karls-Universität Heidelberg, Heidelberg, Germany*
[20]*School of Physics, University College Dublin, Dublin, Ireland*
[21]*INFN Sezione di Bari, Bari, Italy*
[22]*INFN Sezione di Bologna, Bologna, Italy*
[23]*INFN Sezione di Ferrara, Ferrara, Italy*
[24]*INFN Sezione di Firenze, Firenze, Italy*
[25]*INFN Laboratori Nazionali di Frascati, Frascati, Italy*
[26]*INFN Sezione di Genova, Genova, Italy*
[27]*INFN Sezione di Milano, Milano, Italy*
[28]*INFN Sezione di Milano-Bicocca, Milano, Italy*
[29]*INFN Sezione di Cagliari, Monserrato, Italy*
[30]*INFN Sezione di Padova, Padova, Italy*
[31]*INFN Sezione di Perugia, Perugia, Italy*
[32]*INFN Sezione di Pisa, Pisa, Italy*
[33]*INFN Sezione di Roma La Sapienza, Roma, Italy*
[34]*INFN Sezione di Roma Tor Vergata, Roma, Italy*
[35]*Nikhef National Institute for Subatomic Physics, Amsterdam, Netherlands*
[36]*Nikhef National Institute for Subatomic Physics and VU University Amsterdam, Amsterdam, Netherlands*
[37]*AGH—University of Krakow, Faculty of Physics and Applied Computer Science, Kraków, Poland*
[38]*Henryk Niewodniczanski Institute of Nuclear Physics Polish Academy of Sciences, Kraków, Poland*
[39]*National Center for Nuclear Research (NCBJ), Warsaw, Poland*
[40]*Horia Hulubei National Institute of Physics and Nuclear Engineering, Bucharest-Magurele, Romania*
[41]*Affiliated with an institute covered by a cooperation agreement with CERN*
[42]*DS4DS, La Salle, Universitat Ramon Llull, Barcelona, Spain*
[43]*ICCUB, Universitat de Barcelona, Barcelona, Spain*
[44]*Instituto Galego de Física de Altas Enerxías (IGFAE), Universidade de Santiago de Compostela, Santiago de Compostela, Spain*
[45]*Instituto de Fisica Corpuscular, Centro Mixto Universidad de Valencia—CSIC, Valencia, Spain*
[46]*European Organization for Nuclear Research (CERN), Geneva, Switzerland*
[47]*Institute of Physics, Ecole Polytechnique Fédérale de Lausanne (EPFL), Lausanne, Switzerland*
[48]*Physik-Institut, Universität Zürich, Zürich, Switzerland*
[49]*NSC Kharkiv Institute of Physics and Technology (NSC KIPT), Kharkiv, Ukraine*
[50]*Institute for Nuclear Research of the National Academy of Sciences (KINR), Kyiv, Ukraine*
[51]*University of Birmingham, Birmingham, United Kingdom*
[52]*H. H. Wills Physics Laboratory, University of Bristol, Bristol, United Kingdom*
[53]*Cavendish Laboratory, University of Cambridge, Cambridge, United Kingdom*
[54]*Department of Physics, University of Warwick, Coventry, United Kingdom*
[55]*STFC Rutherford Appleton Laboratory, Didcot, United Kingdom*
[56]*School of Physics and Astronomy, University of Edinburgh, Edinburgh, United Kingdom*
[57]*School of Physics and Astronomy, University of Glasgow, Glasgow, United Kingdom*
[58]*Oliver Lodge Laboratory, University of Liverpool, Liverpool, United Kingdom*
[59]*Imperial College London, London, United Kingdom*
[60]*Department of Physics and Astronomy, University of Manchester, Manchester, United Kingdom*
[61]*Department of Physics, University of Oxford, Oxford, United Kingdom*
[62]*Massachusetts Institute of Technology, Cambridge, Massachusetts, USA*
[63]*University of Cincinnati, Cincinnati, Ohio, USA*
[64]*University of Maryland, College Park, Maryland, USA*
[65]*Los Alamos National Laboratory (LANL), Los Alamos, New Mexico, USA*
[66]*Syracuse University, Syracuse, New York, USA*
[67]*Pontifícia Universidade Católica do Rio de Janeiro (PUC-Rio), Rio de Janeiro, Brazil (associated with Universidade Federal do Rio de Janeiro (UFRJ), Rio de Janeiro, Brazil)*

[68]School of Physics and Electronics, Hunan University, Changsha City, China (associated with Institute of Particle Physics, Central China Normal University, Wuhan, Hubei, China)
[69]Guangdong Provincial Key Laboratory of Nuclear Science, Guangdong-Hong Kong Joint Laboratory of Quantum Matter, Institute of Quantum Matter, South China Normal University, Guangzhou, China (associated with Center for High Energy Physics, Tsinghua University, Beijing, China)
[70]Lanzhou University, Lanzhou, China (associated with Institute of High Energy Physics (IHEP), Beijing, China)
[71]School of Physics and Technology, Wuhan University, Wuhan, China (associated with Center for High Energy Physics, Tsinghua University, Beijing, China)
[72]Departamento de Fisica, Universidad Nacional de Colombia, Bogota, Colombia (associated with LPNHE, Sorbonne Université, Paris Diderot Sorbonne Paris Cité, CNRS/IN2P3, Paris, France)
[73]Universität Bonn—Helmholtz-Institut für Strahlen und Kernphysik, Bonn, Germany (associated with Physikalisches Institut, Ruprecht-Karls-Universität Heidelberg, Heidelberg, Germany)
[74]Eotvos Lorand University, Budapest, Hungary (associated with European Organization for Nuclear Research (CERN), Geneva, Switzerland)
[75]Van Swinderen Institute, University of Groningen, Groningen, Netherlands (associated with Nikhef National Institute for Subatomic Physics, Amsterdam, Netherlands)
[76]Universiteit Maastricht, Maastricht, Netherlands (associated with Nikhef National Institute for Subatomic Physics, Amsterdam, Netherlands)
[77]Tadeusz Kosciuszko Cracow University of Technology, Cracow, Poland (associated with Henryk Niewodniczanski Institute of Nuclear Physics Polish Academy of Sciences, Kraków, Poland)
[78]Universidade da Coruña, A Coruna, Spain (associated with DS4DS, La Salle, Universitat Ramon Llull, Barcelona, Spain)
[79]Department of Physics and Astronomy, Uppsala University, Uppsala, Sweden (associated with School of Physics and Astronomy, University of Glasgow, Glasgow, United Kingdom)
[80]University of Michigan, Ann Arbor, Michigan, USA (associated with Syracuse University, Syracuse, New York, USA)
[81]Departement de Physique Nucleaire (SPhN), Gif-Sur-Yvette, France

[a]Deceased.
[b]Also at Università di Milano Bicocca, Milano, Italy.
[c]Also at Università di Roma Tor Vergata, Roma, Italy.
[d]Also at Università di Firenze, Firenze, Italy.
[e]Also at Università di Ferrara, Ferrara, Italy.
[f]Also at Università di Padova, Padova, Italy.
[g]Also at Università di Bologna, Bologna, Italy.
[h]Also at Università di Genova, Genova, Italy.
[i]Also at Università degli Studi di Milano, Milano, Italy.
[j]Also at Universidad Nacional Autónoma de Honduras, Tegucigalpa, Honduras.
[k]Also at Università di Cagliari, Cagliari, Italy.
[l]Also at Centro Federal de Educacão Tecnológica Celso Suckow da Fonseca, Rio De Janeiro, Brazil.
[m]Also at Università di Bari, Bari, Italy.
[n]Also at Università di Perugia, Perugia, Italy.
[o]Also at LIP6, Sorbonne Universite, Paris, France.
[p]Also at Universidade de Brasília, Brasília, Brazil.
[q]Also at Università di Pisa, Pisa, Italy.
[r]Also at Hangzhou Institute for Advanced Study, UCAS, Hangzhou, China.
[s]Also at Scuola Normale Superiore, Pisa, Italy.
[t]Also at School of Physics and Electronics, Henan University, Kaifeng, China.
[u]Also at Excellence Cluster ORIGINS, Munich, Germany.
[v]Also at Universita degli studi di Bergamo, Bergamo, Italy.
[w]Also at Department of Physics/Division of Particle Physics, Lund, Sweden.
[x]Also at Università della Basilicata, Potenza, Italy.
[y]Also at Università di Siena, Siena, Italy.
[z]Also at Universidad de Alcalá, Alcalá de Henares, Spain.
[aa]Also at Università di Urbino, Urbino, Italy.